LAWRENCE
LIVERMORE
NATIONAL
LABORATORY

LLNL-TR-413222

# Development of Fiber Laser Weld Parameters for Stainless Steel and Refractory Metals

J. Elmer, R. Pong

May 21, 2009

**Disclaimer**

This document was prepared as an account of work sponsored by an agency of the United States government. Neither the United States government nor Lawrence Livermore National Security, LLC, nor any of their employees makes any warranty, expressed or implied, or assumes any legal liability or responsibility for the accuracy, completeness, or usefulness of any information, apparatus, product, or process disclosed, or represents that its use would not infringe privately owned rights. Reference herein to any specific commercial product, process, or service by trade name, trademark, manufacturer, or otherwise does not necessarily constitute or imply its endorsement, recommendation, or favoring by the United States government or Lawrence Livermore National Security, LLC. The views and opinions of authors expressed herein do not necessarily state or reflect those of the United States government or Lawrence Livermore National Security, LLC, and shall not be used for advertising or product endorsement purposes.

This work performed under the auspices of the U.S. Department of Energy by Lawrence Livermore National Laboratory under Contract DE-AC52-07NA27344.

# Development of Fiber Laser Weld Parameters for Stainless Steel and Refractory Metals

John W. Elmer and Randy Pong

May 20, 2009

## Summary

Laser welds were made in 21-6-9 stainless steel, vanadium and tantalum using LLNL's new 6kW fiber laser to target 1 mm penetration depths. The materials were machined into flat coupon samples with standard step-joint geometries, and were welded in a continuous wave mode. The laser was characterized using the Primes laser beam diagnostic system so that the beams can be reproduced in the future. The optical configuration consisted of a 200 μm fiber, 200 mm collimator and 250 mm focusing lens, which delivered electron-beam level power densities in the 5 to 20 kW/mm$^2$ range. The three different materials required different power densities to produce the desired penetration, and this report summarizes the results of this screening study that was directed at developing a first approximation to the proper welding parameters for future work. The results show that 1 mm penetrations can be achieved using a 400W beam for 21-6-9 stainless steel, a 600W beam for vanadium, and a 1,100W beam for tantalum using sharp focus and a travel speed of 40 inch/min. Future welds should incorporate a trailing gas shield to prevent discoloration of the surface and to prevent oxygen and nitrogen pickup in the welds.

## Background

Laser beam parameters are being developed to weld vanadium, 21-6-9 stainless steel and tantalum using the new 6 kW IPG fiber laser at LLNL. This laser can produce electron-beam level power densities, and can be delivered through a number of optical configurations. These optics combinations include three different fiber diameters (200, 300 and 400 μm), two different collimators (160 and 200 mm) and three different focusing lenses (160, 200 and 250 mm). The Primes laser diagnostic unit was recently used to characterize the laser beam for different optics configurations [1]. The previous work measured the beam radius and beam quality ($M^2$, Rayleigh length, beam parameter product) as a function of defocus condition for 12 of the 18 possible optical configurations. The results showed that the measured power densities are in the 5 to 30 kW/mm$^2$ range for the set of parameters investigated, and that the 200 μm fiber matched electron beam power densities at the kW level nearly exactly when using the 250 mm focusing lens. Based on the diagnostic results, a 200 μm fiber, 200 mm collimator and 250 mm focusing lens combination was chosen as the baseline setup for the first set of practice welds, and

this report summarizes the results of the welds that were made on flat coupons of vanadium, tantalum and 21-6-9 stainless steel using well characterized laser beams.

## Experimental Procedures

### IPG Fiber Laser Welder and Laser Beam Characterization

The new IPG laser is shown in Fig. 1 and was fully integrated into the existing Rofin Sinar workstation in late 2008. Each fiber goes directly from the IPG laser to the collimator that is located at the top of the workstation, see Fig. 1. The beam is then bent by a 90 deg mirror and passes through a quartz window to enter the workstation, where it travels approximately 24 inches before entering the final focusing optic assembly. This assembly consists of two 90 deg. mirrors for beam articulation that are mounted above the focusing lens assembly as shown in Fig. 2. An air knife is present below the lens assembly to help minimize metal vapors form depositing on the cover slide below the lens.

Laser beam characterization performed previously indicated that a 200μm fiber, 200mm collimator and 250 mm lens combination matched closely with electron beams used at the 1-kW level [1]. In the present study, this optics combination was used, and the beams were characterized just prior to making the welds. The Primes diagnostic unit (model FM 120 SN1202) was used to measure the power density distribution over a 14 mm range of travel along the propagation direction of the beam (Z-axis). The diagnostic uses a rapidly spinning hollow needle technique to sample the beam where it is analyzed using a photodiode detector. In these experiments a High Div YAG probe tip manufactured by Primes with a designated pinhole diameter of 18x22 μm and sensitivity of 1200 cts/(MW/cm$^2$) was used (serial number Y-435). The needle was rotated at 3750 RPM, and helium gas was kept flowing through the needle to keep it from overheating. Note that the sensor sensitivity was set on “Low” rather than “High” in this study, which seemed to prevent the saturation of the sensor at high powers. This setting change, using the slide switch on the sensor (see Fig 3), eliminated the problems we were seeing previously with apparent increases in the beam diameter as the power increased to the kW level [1]. A photograph of the diagnostic unit is also shown in Fig. 3 where it is mounted directly above a water cooled beam dump (Laser Mechanisms Beam Absorber Model PLBPD 0010) to absorb the laser power.

The Primes diagnostic was used to take 15 planes of data over a 14 mm span across the beam waist. This data is fit using a “caustic” analysis that represents the beam convergence and divergence along a plane parallel to the beam propagation axis. The results of the analysis mathematically fit the data using the Primes software (version 2.73) in order to determine the beam quality ($M^2$, Rayleigh length, beam parameter product) based on a “second moment” calculation [1]. This technique was used to characterize the laser from power levels between 200W and 1200W, and the results from each beam are presented in the Appendix. This compilation of data shows the characteristics of each beam, including pseudo-color images of the beam intensities, and cross sectional profiles through each beam in two orthogonal directions. These data are further summarized in Table 1, which compares the beam radii and beam quality parameters for each of the laser beams. The results are plotted in Figure 4, which gives the beam quality parameters and beam radius as a function of laser power level. The beam

quality is relatively constant over this range, and the results show that the beam radius is 0.142mm +- 0.002 mm for the range of powers investigated. This relatively constant beam radius results in a linear increase in the beam's power density with increasing power, from 3.1 to 19.2 kW/mm2, which is similar to the power densities of kW level electron beams used to weld these same materials at LLNL in the past. For example, a typical electron beam used for welding was characterized to have an average power density of 10.5kW/mm$^2$ for an 840W sharp focused beam, and had a measured radius of 0.159 mm [2].

## Materials and Laser Beam Welding Experiments

Vanadium, tantalum and 21-6-9 stainless steel all respond differently to laser beams used for welding because of their differences in density, melting points and thermal properties [3]. Because of this, these three materials are ideal for testing the variations in penetration and fusion zone geometry that can occur during welding. Coupons from each of these materials were machined from existing in-house 6-mm thick sheet (vanadium and tantalum) and in-house 18 mm thick bar (21-6-9 SS), identical to the compositions used in previous experiments [3]. The coupons measured 6 inch long, 1 inch wide and were approximately 0.060 inch (1.5 mm) thick. The joint design consisted of a standard step-joint geometry to simulate welds where the required penetration is on the order of 1 mm.

Based on the results of previous laser welding studies on stainless steel and refractory metals using a 2kW diode-pumped NdYAG laser at LLNL [3], we chose a range of welding powers that spanned approximately 2X for each of the three materials to make sure that we spanned the desired 1mm penetration point at 40 ipm travel speed. Table 2 summarizes the power levels used and the power density produced by each beam. This range of powers was chosen as a starting point in order to gage the response of each of the three materials to the new laser. The different powers used to weld each material are highlighted in Figure 5, on a plot of laser power versus average power density of the beam, where the Average Power Density = Power/$\pi$*R$^2$, where R is the measured beam radius. The approximate linear increase in power density with laser power is the result of the relatively constant beam radius.

The welds were made by clamping the flat coupon in an aluminum hold-down fixture. A copper strip was placed directly below the weld joint to act as a heat sink. The welds were all made at 40 inch/min (16.9 mm/s) using a sharp focused beam and the 200 $\mu$m fiber, 200 mm collimator, and 250 mm lens, with the beam positioned normal to the surface being welded. A single shielding gas nozzle was directed from the front to the back of the weld along the weld centerline, which flowed argon gas at the beam impingement point to assist with removal of the laser plasma plume. An exhaust trunk was placed behind the weld to remove the weld-generated vapors. No further shielding gas arrangements were implemented in this study.

Four welds were made on each coupon, each weld being approximately 1.5 inch long. The laser was set up using 4 of the 16 400Wmodules turned on, giving it a maximum power of 1.6kW, which was sufficient for this set of welds. Reducing the number of modules gives better accuracy for the lower power welds, which should not be less than 10% of the maximum value. Continuous wave welds were made with no slope in or slope out, allowing the weld to quickly come up to steady state and allowing the weld crater

to be examined as it would appear during welding. After welding, the weld craters were photographed, and the welds were cross sectioned near their mid point. The cross sectioned samples were polished and etched using standard metallographic procedures to determine the weld penetration and geometry. In addition, the vanadium samples were inspected using microhardness measurements to compare them to electron beam welds made in vacuum on the same material [2].

## Results and Discussion

### *Weld Crater Shape*

Before cross sectioning the welded samples, the crater (tail end) of each weld was photographed on the top surface to get an indication of the size of the liquid weld pool, and an indication of the size of the ripple marks on the surface of the welds. Fig 6 shows the craters in the 21-6-9 stainless steel, Fig 7 shows the craters in the vanadium welds, and Fig 8 shows the craters in the tantalum welds. The scale markers in all photographs are the same with 1 mm increments. Discoloration of the surface occurred in most of the welds, with the intensity generally increasing with increasing power level of the beam. This discoloration is undesirable, and future welds will require a trailing gas shield and longer purge times with the argon gas to prevent oxidation.

Measurements of the crater dimensions were made parallel to the welding direction, designated as "X", and perpendicular to the welding direction, designated as "Y". These measurements are summarized in Table 2 and are plotted in Fig. 9. The dimensions of the craters follow the expected trend with power, showing that the crater increases in size with increasing power. For 21-6-9 SS and vanadium, there is a large jump in crater size between the lowest and next to lowest power levels, indicating that the laser most likely did not couple well with the materials at the lowest power level and thus absorbed a smaller fraction of the beam's energy. In the case of the 21-6-9 SS and vanadium, the X-dimension of the crater deviated to higher values with increasing power, as the weld pool takes on an elongated shape. At the highest power for the 21-6-9 SS (500W), the weld began to take on a tear-drop shape and its length appears to deviate from the trend at lower powers. This was the only weld in the group that showed complete penetration through the coupon thickness. For tantalum, the X and Y-dimensions were nearly identical for all power levels, indicating that the weld pool retained a circular shape all the way up to 1200 W power. The largest difference in crater shape was due to that material itself, where the smallest craters were formed in the tantalum and the largest in the 21-6-9 SS for a given power level.

### *Weld Penetration and Width*

The 12 welds were cross sectioned at the mid weld distance and metallographically prepared using conventional techniques, and etched in either oxalic acid (21-6-9 SS), ASTM etchant 163 (vanadium), or 10% $FeCl_3$ (tantalum). The cross sections were then photographed so that the weld penetrations could be measured. These data are also summarized in Table 2.

The metallographic cross sections for the 21-6-9 SS welds are shown in Fig. 10. At the lowest power of 200W the melt pool is shallow and wide, indicating that that laser is not keyholing and may not be

absorbing the beam's total power. As the power is increased to 300W, a deeper penetrating central portion of the beam appears, indicating that a keyhole is beginning to form. At 400W, the penetration is now down to the bottom of the step in the joint, and the weld geometry indicates a blunt keyhole shape. At 500W, the penetration is very deep and displays a clear keyhole shape. All of the welds are free of porosity and do not have any cracks. Based on these samples, the 400W beam would be an ideal choice for producing a 1 mm deep weld in 21-6-9 stainless steel.

The metallographic cross sections for the vanadium welds are shown in Fig. 11. At the lowest power of 300W, the beam hardly penetrates the material and there is no fusion across the joint. The near complete lack of penetration indicates that the laser beam did not couple well with the vanadium at this power density. At 400W, the beam penetrates the vanadium part way to the step and creates a nice looking weld, but has less than 1 mm penetration. At 500W, the penetration is clearly to the step and at 600W the penetration is below the step. Due to the large amount of grain growth in the heat affected zone of vanadium, the fusion boundary is difficult to discern. However, it is clear that the welds are free of porosity and cracks. Based on these samples, a power level of 600W would be used for producing 1 mm deep welds in vanadium.

The metallographic cross sections for the tantalum welds are shown in Fig. 12. At the lowest power level of 600W, the penetration is very shallow and only a small amount of material is melted. At this power level it appears that the beam is not coupling well with tantalum and a large fraction of the beam is not being absorbed. At 800W, the beam penetrates approximately half way to the step, and it contains one small void. At 1000W, the beam penetrates nearly to the step and contains 2 small voids. At the highest power of 1200W, the beam penetrates to the step, with penetrations slightly in excess of 1mm, and contains a medium sized void at the root of the weld. Although these welds contain some porosity, it is much smaller than the porosity observed in laser welds in tantalum made with the lower power density beams on the old Rofin Sinar laser [3]. This type of porosity is related to keyhole collapse, and is related to the high density of the tantalum. The porosity is less severe in these welds due to the higher power densities produced by the new laser ant eh 0.200 mm fiber, as compared to the 0.300 mm fiber with the previous laser. Based on these samples, a power level of 1,100 kW would be selected for 1mm penetrations in tantalum.

Figure 13 summarizes the weld penetration study results by plotting the penetration depths versus laser power in each of the three materials. It is clear that each of the three materials responds quite differently to the laser, whereby 21-6-9 SS, vanadium and tantalum respectively require higher powers to reach 1 mm penetration. While the 21-6-9 stainless steel and vanadium increase penetration nearly linearly over this power range, tantalum, with its much higher density and melting point, shows a decreasing rate of penetration with power. Future welds in tantalum would most likely benefit from a higher power density beam produced by a smaller focal length lens and/or a larger collimator size.

***Weld Microhardness***

The discoloration of the weld surfaces indicated that the shielding gas coming from the front of the weld and through the nozzle was insufficient for this first set of laser welds. Although the discoloration itself

is not a concern, the probability of drawing air in to the weld fusion zone is high. The underlying concern is that the mechanical properties of the tantalum and vanadium samples might be adversely affected, since oxygen and nitrogen impurities increase the yield strength and decrease the ductility of these refractory metals. The 21-6-9SS is less of a concern since it is an iron-based multi-phase alloy that can tolerate small amounts of oxygen and nitrogen without significant changes in properties.

Microhardness measurements were made on the 1 mm deep laser welds to compare the hardness of the fusion zone to that of the base metal. This comparison provides an indication of any changes caused by the welding, and will be used as a base line for future welds in these materials. The microhardness measurements were made on the polished weld cross sections, using a 50gmf load and a calibrated Vickers hardness tester. Six measurements were made on each sample in both the weld and in the fusion zone, and the results are summarized in Table 3. The microhardness values for the vanadium increased from 105 HVN in the base metal to 137 in the weld zone. This is a significant increase, and attempts should be made to minimize hardness increases in future welds. However, this hardness is not considered to be a problem, since this material is still relatively soft compared to vanadium laser welds made in air with no shielding gas that are brittle and can have hardness values as high as 567 VHN [4]. The microhardness values of the tantalum also showed an increase from 99.5 VHN in the base metal to 116 VHN in the weld, which is similar to the changes seen in the vanadium welds for the same reasons. The 21-6-9 SS on the other hand, showed a decrease in hardness from 235 VHN to 221 VHN. This result could be due to the larger grain size in the fusion zone of the 21-6-9SS welds, but this difference may not be statistically significant.

Table 3 further compares the hardness values of the vanadium and 21-6-9SS laser welds and base metals with electron beam welds and base metals from a previous study [2]. These results indicate that the base metals used for the laser welds started approximately 10 VHN higher than those of the electron beam study. The vanadium EB welds also increased in hardness, but showed less of an increase than the laser welds. This observation indicates that the laser welds most likely picked up oxygen and/or nitrogen during welding, which resulted in their higher hardness increase as compared to the electron beam welds. The 21-6-9SS EB welds showed a similar decrease in hardness from the base metal as the laser welds.

## Conclusions

The new IPG fiber laser was used to weld 21-6-9 stainless steel, vanadium, and tantalum coupons to develop parameters for achieving penetrations of 1 mm in each material. These welds were characterized using the Primes laser diagnostic showing average power densities in the 5-20 kW/mm2 were required, depending on the material. These power densities are similar to those produced by electron beams used in the past.

All welds were made using sharp focused laser beams produced by a 200 μm diameter fiber, a 250 mm lens and a 200 mm collimator combination, and all welds were made at 40 ipm. The welds were essentially defect free, except for the tantalum that contained some porosity in the higher power welds.

This porosity is likely due to keyhole collapse in the dense tantalum, and could potentially be prevented by using higher power density beams that can easily be produced with this laser using a different optical configuration. Oxidation of the weld surface was observed on most of the samples, and is due to insufficient shielding gas, which was expected since no attempts were made in this study to prevent oxidation. The insufficient shielding gas had a minor effect on the hardness of the vanadium and tantalum samples, and is considered to be only a minor concern. Future welds will be performed with a trailing gas shield to protect the weld surface in an attempt to minimize the discoloration on the weld surface and reduce the amount of oxygen and nitrogen in the weld fusion zone.

Based on the results of this study, it is recommended that future welds in these materials use baseline laser welding parameters of 400W for the 21-6-9 SS, 600W for the vanadium, and 1100W for the tantalum to produce 1 mm deep welds. A trailing gas shield should be designed and fabricated for future welds to help minimize oxygen and nitrogen pickup. If porosity in the tantalum is a concern then a higher power density beam would be recommended, which can be accomplished by using a shorter focal length lens, a larger collimator, and/or higher beam powers moving at higher speeds.

## Acknowledgement

This work performed under the auspices of the U.S. Department of Energy by Lawrence Livermore National Laboratory under Contract DE-AC52-07NA27344. This document was prepared as an account of work sponsored by an agency of the United States government. Neither the United States government nor Lawrence Livermore National Security, LLC, nor any of their employees makes any warranty, expressed or implied, or assumes any legal liability or responsibility for the accuracy, completeness, or usefulness of any information, apparatus, product, or process disclosed, or represents that its use would not infringe privately owned rights. Reference herein to any specific commercial product, process, or service by trade name, trademark, manufacturer, or otherwise does not necessarily constitute or imply its endorsement, recommendation, or favoring by the United States government or Lawrence Livermore National Security, LLC. The views and opinions of authors expressed herein do not necessarily state or reflect those of the United States government or Lawrence Livermore National Security, LLC, and shall not be used for advertising or product endorsement purposes.

## References


1. J. W. Elmer and R. Pong, “A First Look at Using Laser Diagnostics to Characterize High Brightness 6kW Yb:YAG Fiber Laser Beams,” *Lawrence Livermore National Laboratory,* Technical Report LLNL-TR-411661, April 1, 2009.

2. J. W. Elmer, “Characterization of Defocused Electron Beams and Welds in Stainless Steel and Refractory Metals using the Enhanced Modified Faraday Cup Diagnostic,” *Lawrence Livermore National Laboratory*, Technical Report LLNL-TR-410752, February 23, 2009.

3. T. A. Palmer, J. W. Elmer, R. Pong and M. D. Gauthier, ”Welding of Vanadium, Tantalum, 304L and 21-6-9 Stainless Steels, and Titanium Alloys at Lawrence Livermore National Laboratory using a Fiber Delivered 2.2 kW Diode Pumped CW Nd:YAG Laser,” *Lawrence Livermore National Laboratory*, UCRL-TR-222245, 113 pages, June, 2006.

4. M. J. Strum and L. M. Wagner, “Interstitial Embrittlement in Vanadium Laser Welds,” UCRL-JC-109917, February, 1992.

Table 1: Summary of the beam quality parameters for the 200μm diameter fiber on the LLNL 6kW IPG fiber laser with 4 modules turned on. All measurements were made with the LLNL Primes unit and LLNL probe tip. Helium gas was flowing through needle, the speed was set at 3750 RPM, and sensor was set to the "Low" position. The measured beam radius is 0.142 mm which is slightly higher than the calculated, ideal, value of 0.125 mm for this optical setup.

| Collimator (mm) | Lens (mm) | Power (kW) | Radius SM (mm) | $M^2$ | Rayleigh Length (mm) | BPP (mm-mrad) | Avg. Power Density ($kW/mm^2$) |
|---|---|---|---|---|---|---|---|
| | | | | | | | |
| 200 | 250 | 0.2 | 0.143 | 29.3 | 2.061 | 9.9 | 3.11 |
| | | 0.3 | 0.142 | 29.3 | 2.052 | 9.9 | 4.74 |
| | | 0.4 | 0.143 | 29.4 | 2.069 | 9.9 | 6.23 |
| | | 0.5 | 0.143 | 29.2 | 2.072 | 9.8 | 7.78 |
| | | 0.6 | 0.142 | 29.1 | 2.061 | 9.8 | 9.47 |
| | | 0.8 | 0.141 | 28.7 | 2.067 | 9.7 | 12.81 |
| | | 1.0 | 0.138 | 28.4 | 1.988 | 9.6 | 16.71 |
| | | 1.2 | 0.141 | 29.4 | 2.006 | 9.9 | 19.21 |
| | | | | | | | |
| | | Average | 0.142 | 29.100 | 2.047 | 9.813 | |
| | | Standard Deviation | 0.002 | 0.363 | 0.032 | 0.113 | |

Table 2: Results of the laser welds on vanadium, tantalum and 21-6-9 SS.

| Material | Power | Avg. Power Density | Top Crater Dimensions | | Cross Section |
|---|---|---|---|---|---|
| | (kW) | ($kW/mm^2$) | X (mm) | Y(mm) | Depth (mm) |
| | | | | | |
| 21-6-9 SS | 0.2 | 3.11 | 0.563 | 0.563 | 0.147 |
| | 0.3 | 4.74 | 1.21 | 1.14 | 0.587 |
| | 0.4 | 6.23 | 1.54 | 1.35 | 0.996 |
| | 0.5 | 7.78 | 2.07 | 1.55 | 1.200 |
| | | | | | |
| Vanadium | 0.4 | 6.23 | 0.471 | 0.471 | 0.100 |
| | 0.5 | 7.78 | 1.05 | 1.03 | 0.516 |
| | 0.6 | 9.47 | 1.35 | 1.28 | 1.003 |
| | 0.7 | 11.20 | 1.63 | 1.43 | 1.245 |
| | | | | | |
| Tantalum | 0.6 | 9.47 | 0.380 | 0.380 | 0.154 |
| | 0.8 | 12.81 | 0.839 | 0.839 | 0.682 |
| | 1.0 | 16.71 | 1.25 | 1.24 | 0.917 |
| | 1.2 | 19.21 | 1.55 | 1.54 | 1.042 |

Table 3: Results of the micro-hardness measurements on vanadium, tantalum, and 21-6-9 SS. The laser weld data is from this study with minimal gas shielding, the electron beam weld data is from reference 2 and performed in vacuum. Standard deviations are given for each data set as indicated by "STD".

| Condition | Weld Type | Vanadium (600 W weld) | | 21-6-9 SS (400 W weld) | | Tantalum (1000 W weld) | |
|---|---|---|---|---|---|---|---|
| | | VHN | STD | VHN | STD | VHN | STD |
| | | | | | | | |
| Weld FZ | Laser | 137.2 | 2.0 | 258.0 | 1.60 | 116.0 | 1.31 |
| | E-Beam | 100.4 | 3.53 | 221.1 | 8.95 | N/A | N/A |
| | | | | | | | |
| Base Metal | Laser | 105.0 | 1.05 | 235.0 | 3.54 | 99.5 | 1.14 |
| | E-Beam | 92.1 | 3.36 | 223.4 | 12.5 | N/A | N/A |

Figure 1: Photograph of the new 6kW IPG fiber laser (top) and laser welding workstation that was integrated with the new 6kW IPG laser in 2008 (bottom)

Figure 2: Final optics assembly with two 90 deg. mirrors allowing the beam to be rotated and tilted for final positioning. The air knife assembly is visible below the final focusing lens, and an in line CCD camera is used for initial positioning of the beam and monitoring of the weld.

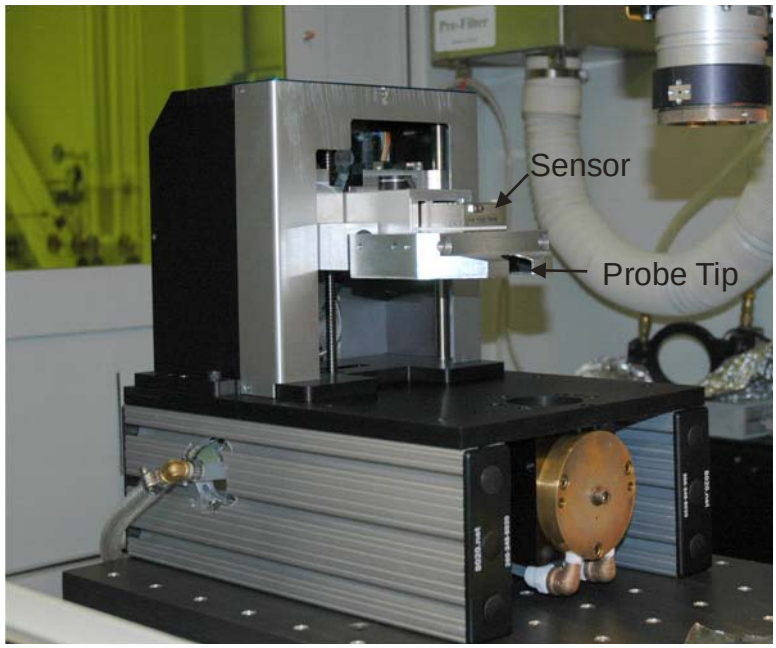


Figure 3: Photo of Primes laser diagnostic unit mounted on top of the water cooled beam dump inside the laser welding workstation. The sensor arrow is pointing to the sensor Low/High switch .

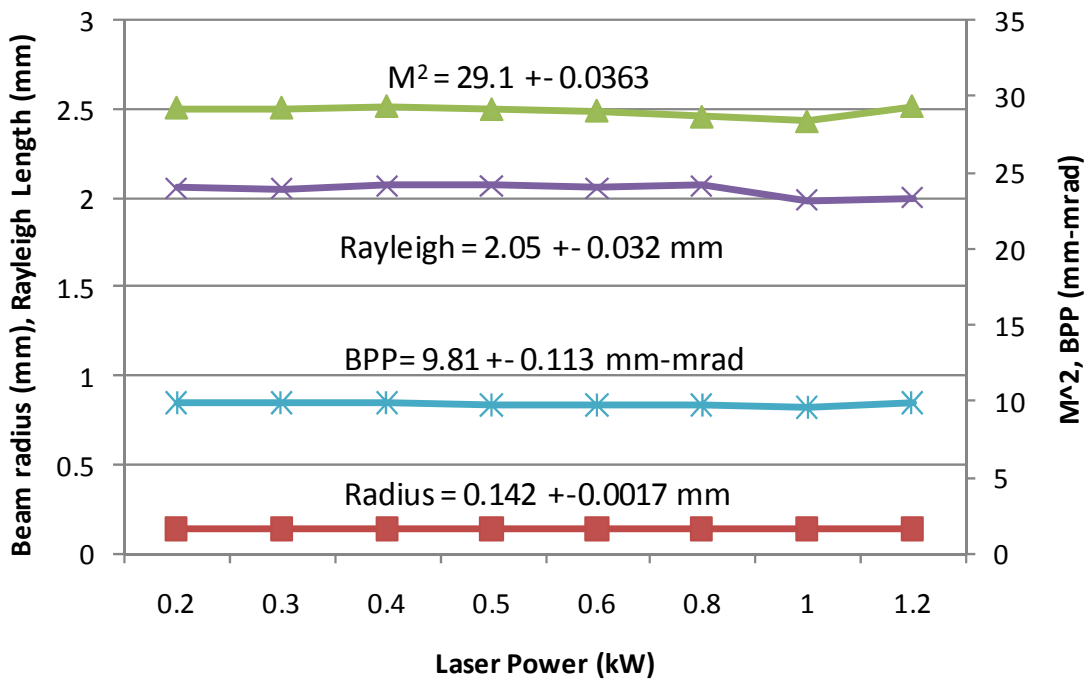


Figure 4: Plot of beam diagnostic measurements for the 200 μm fiber, 200 mm collimator and 250 mm lens up to 1.2 kW beam power. The beam appears to be constant over this power range as indicated by the relatively small standard deviations (± one standard deviation ranges are shown on the plot).

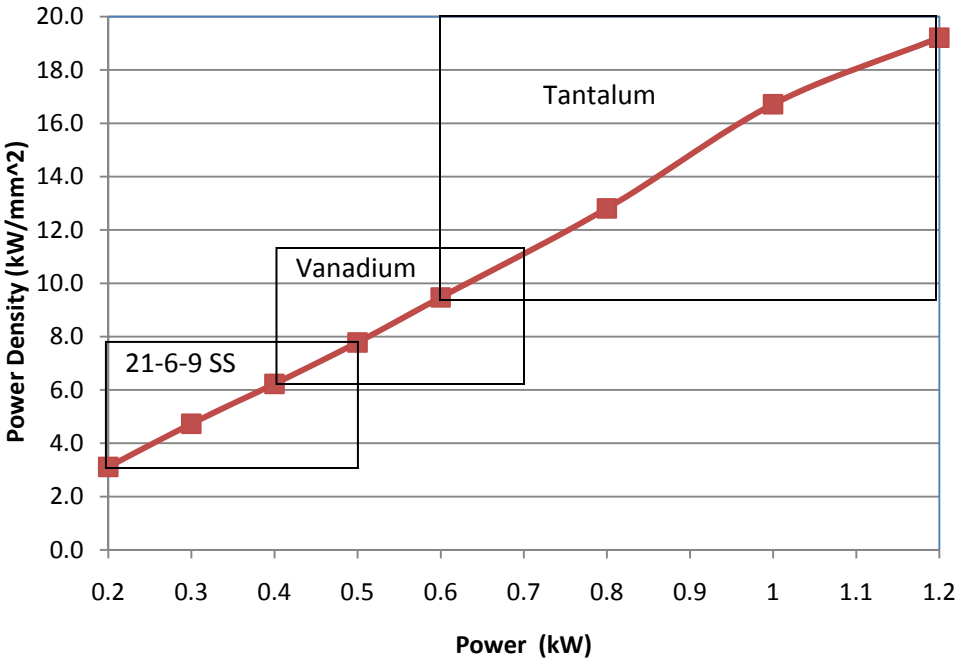


Figure 5: Range of powers used for the coupon welds and associated power densities. The data points and line (red) show the measured power densities for our 6kW IPG fiber laser. 21-6-9 stainless steel requires the least power, vanadium the next highest, and tantalum requires the most power for a given penetration. These power ranges were selected from previous results with our previous 2 kW diode-pumped NdYAG laser welder for a target penetration of 1mm [3].

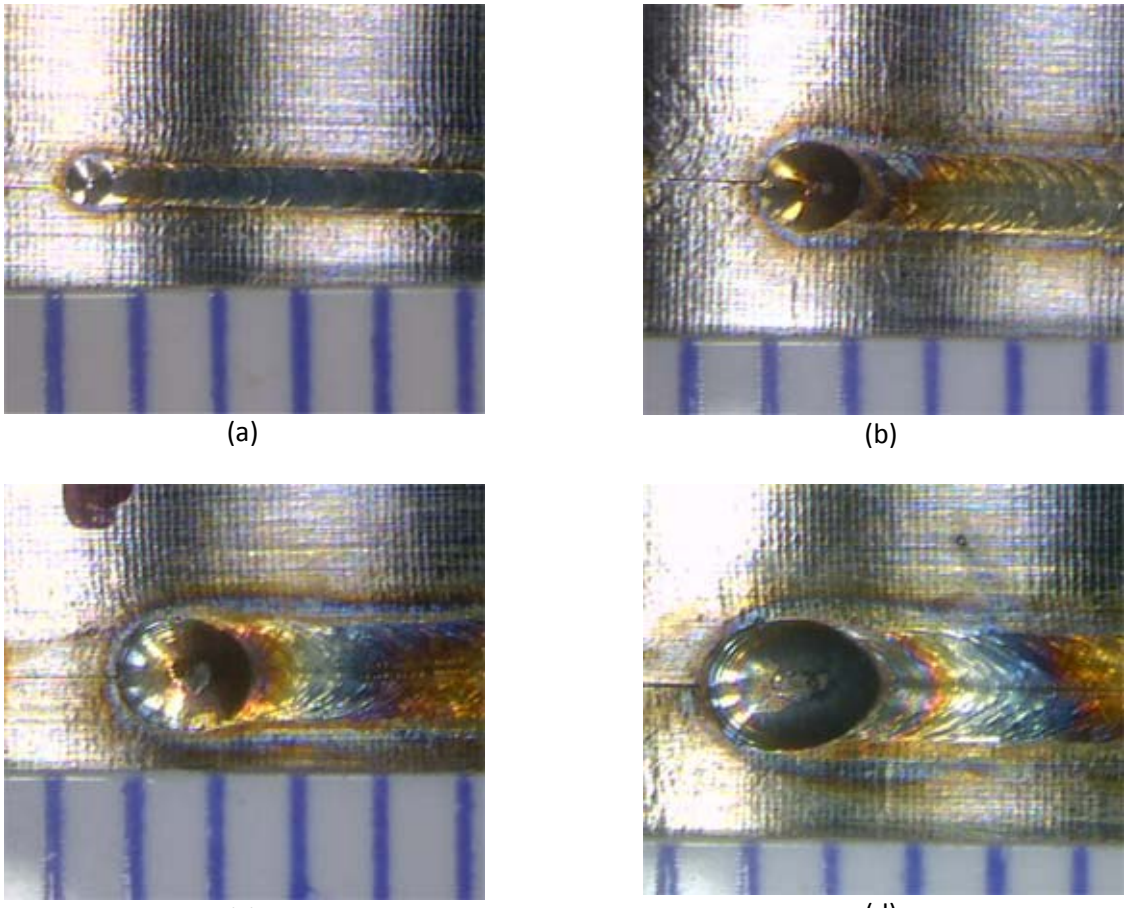

(a) (b) (c) (d)

Figure 6: Macro photographs of the 21-6-9 stainless steel welds made at a) 200W, b) 300W, c) 400W and d) 500 W. All welds were made with sharp focused beams as summarized in Table 1, and were made at 40 ipm. The scale markers are in 1mm increments.

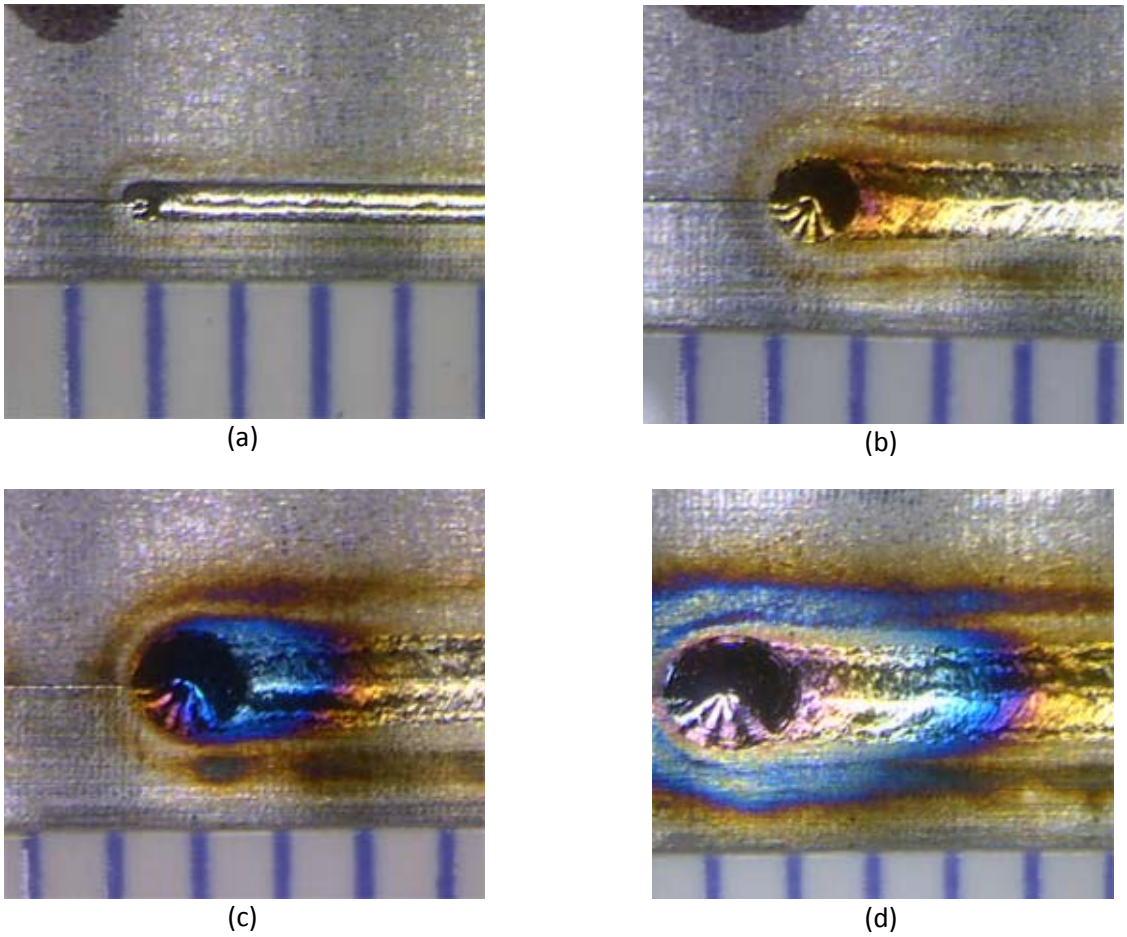


Figure 7: Macro photographs of the vanadium welds made at a) 400W, b) 500W, c) 600W and d) 700 W. All welds were made with sharp focused beams as summarized in Table 1, and were made at 40 ipm. The scale markers are in 1mm increments.

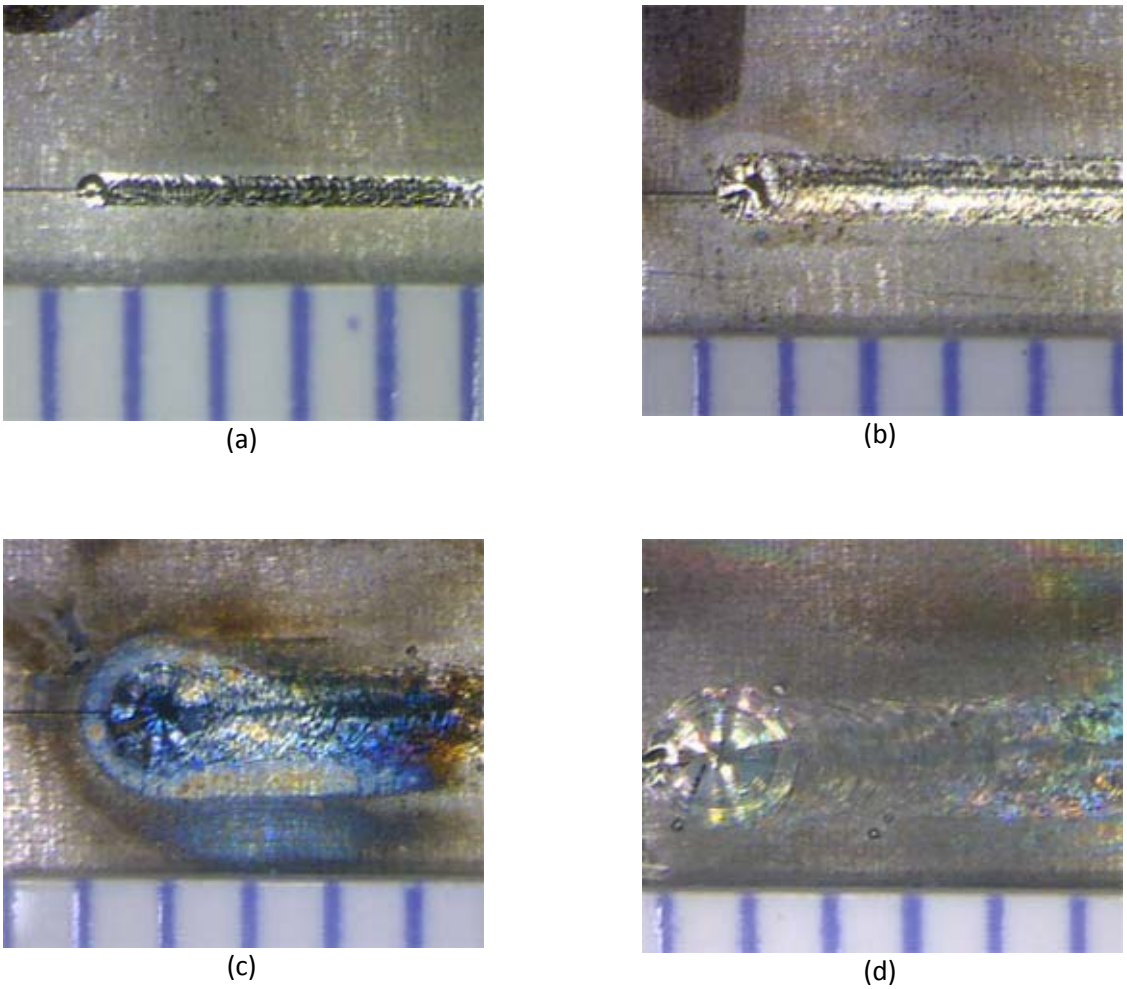


Figure 8: Macro photographs of the vanadium welds made at a) 600W, b) 800W, c) 1000W and d) 1200 W. All welds were made with sharp focused beams as summarized in Table 1, and were made at 40 ipm. The scale markers are in 1mm increments.

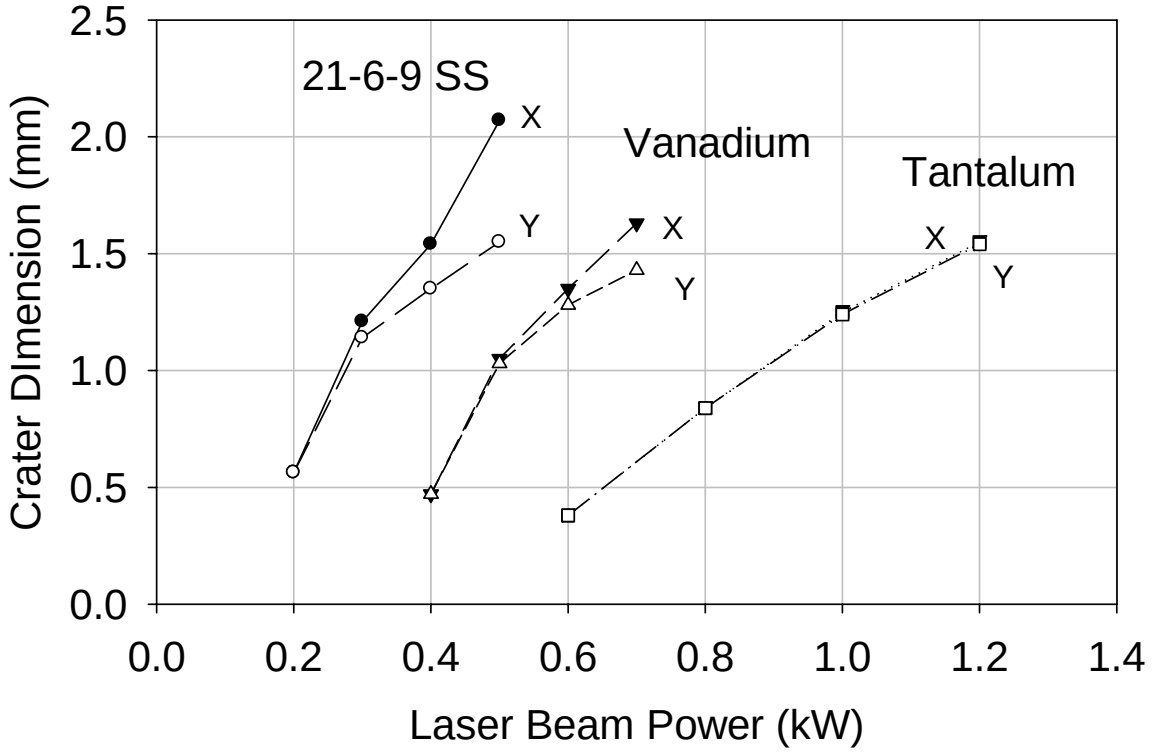


Figure 9: Dimensions of the tail-end craters of each of the 12 welds plotted versus laser power. The X-direction corresponds to the crater length along the welding direction, while the Y-direction corresponds to the crater width perpendicular to the welding direction.

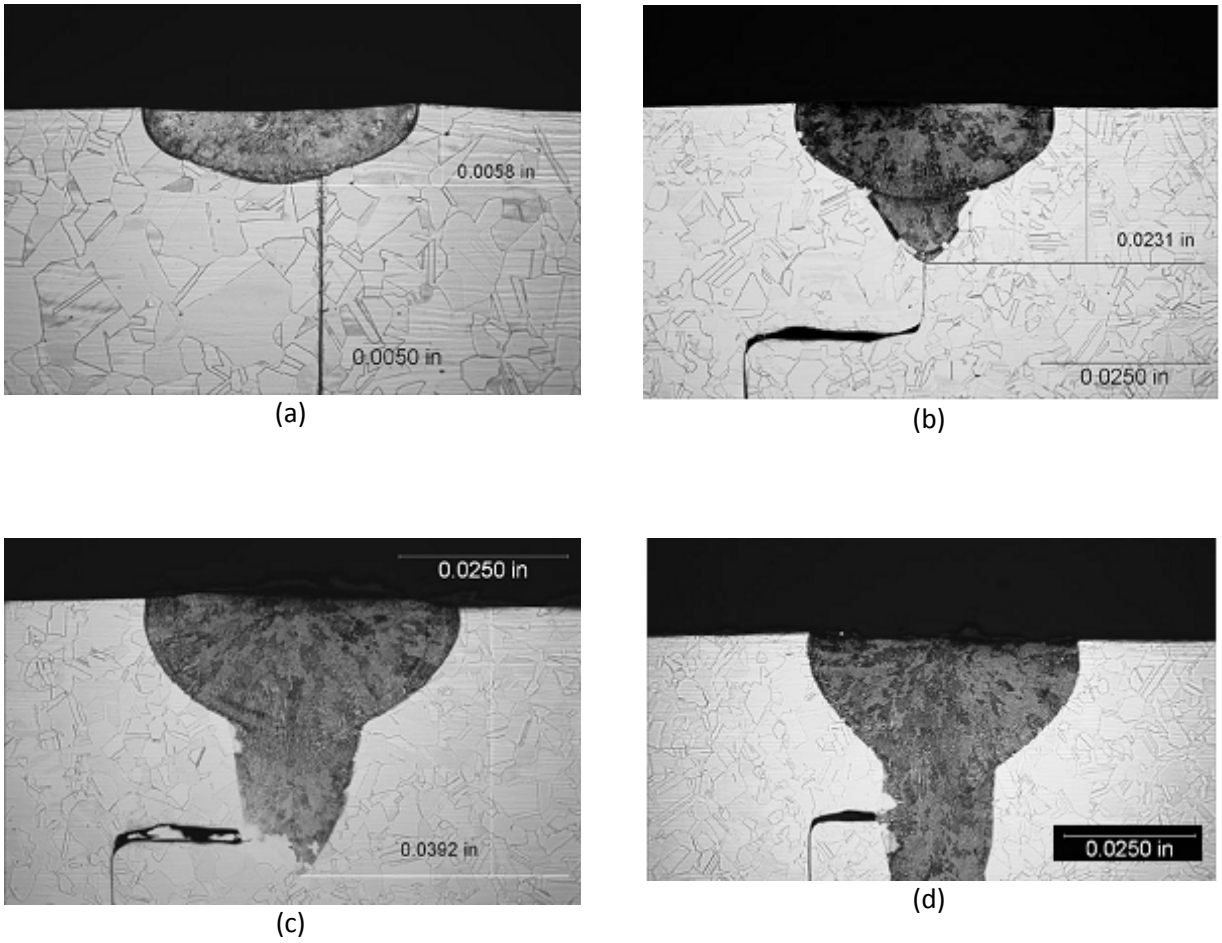


Figure 10: Weld cross sections for the 21-6-9 SS welds. A) 200W, b) 300W, c) 400W and d) 500W. All made at 40 ipm with a sharp focused beam.

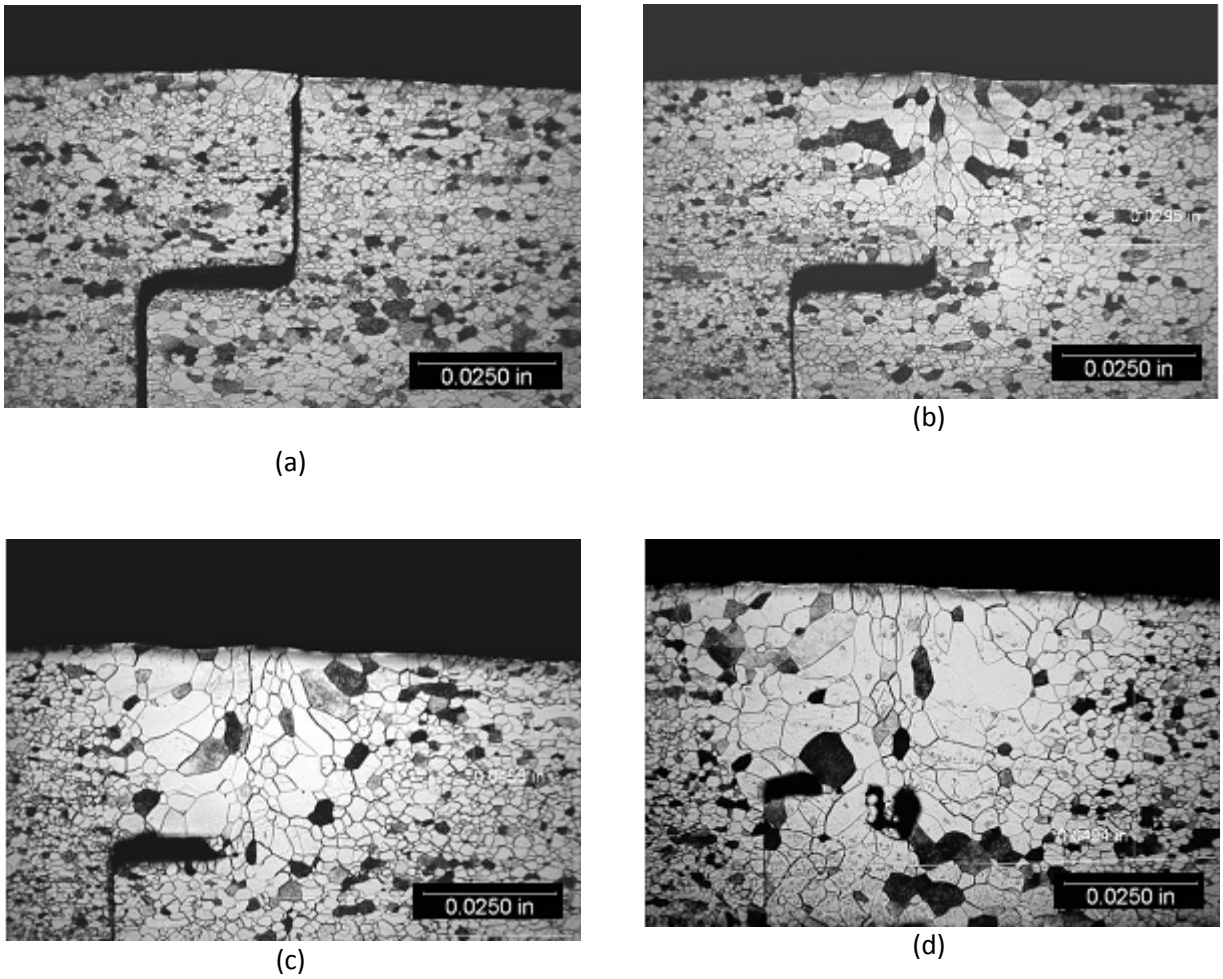


(a) (b) (c) (d)

Figure 11: Weld cross sections for the vanadium welds. A) 400W, b) 500W, c) 600W and d) 700W. All made at 40 ipm with a sharp focused beam.

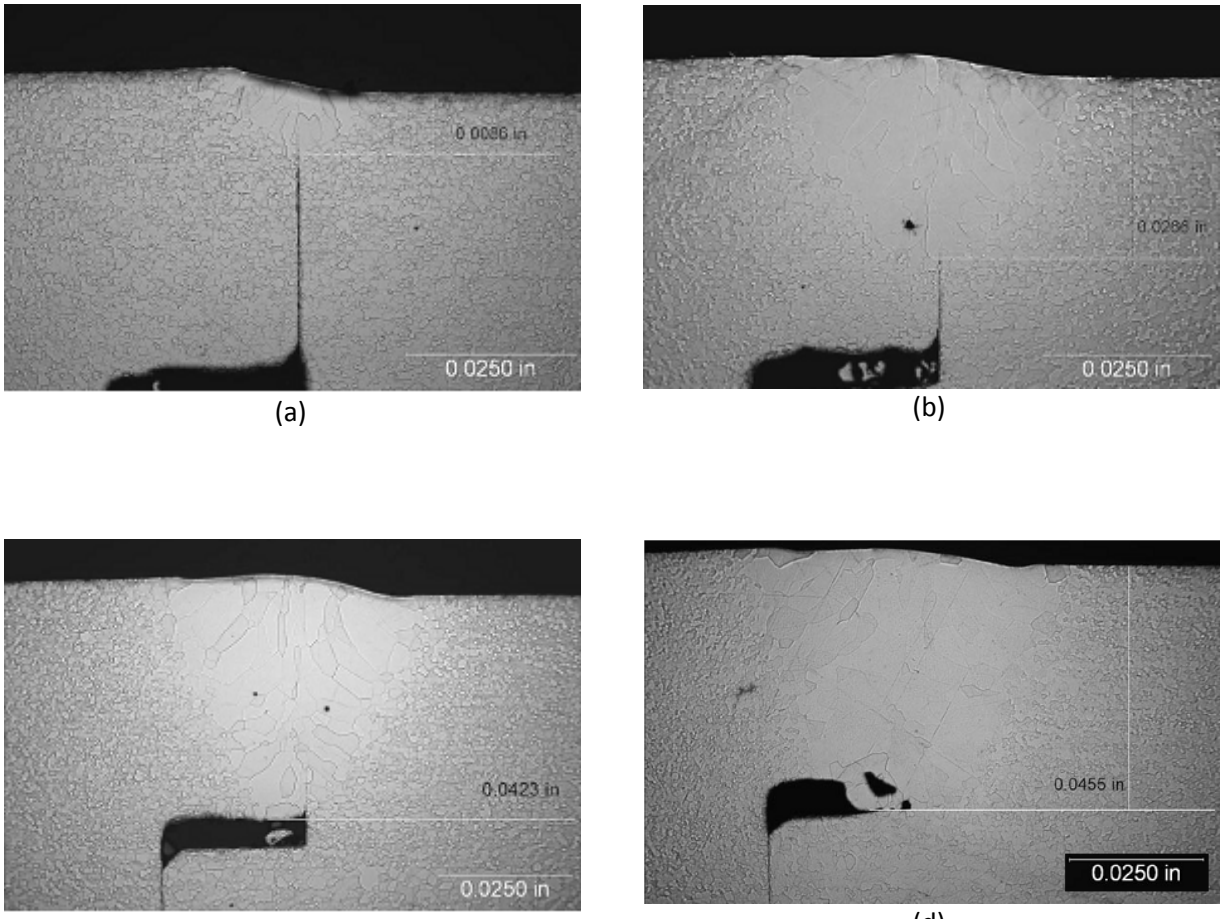


(a) (b) (c) (d)

Figure 12: Weld cross sections for the tantalum welds. A) 600W, b) 800W, c) 1000W and d) 1200W. All made at 40 ipm with a sharp focused beam.

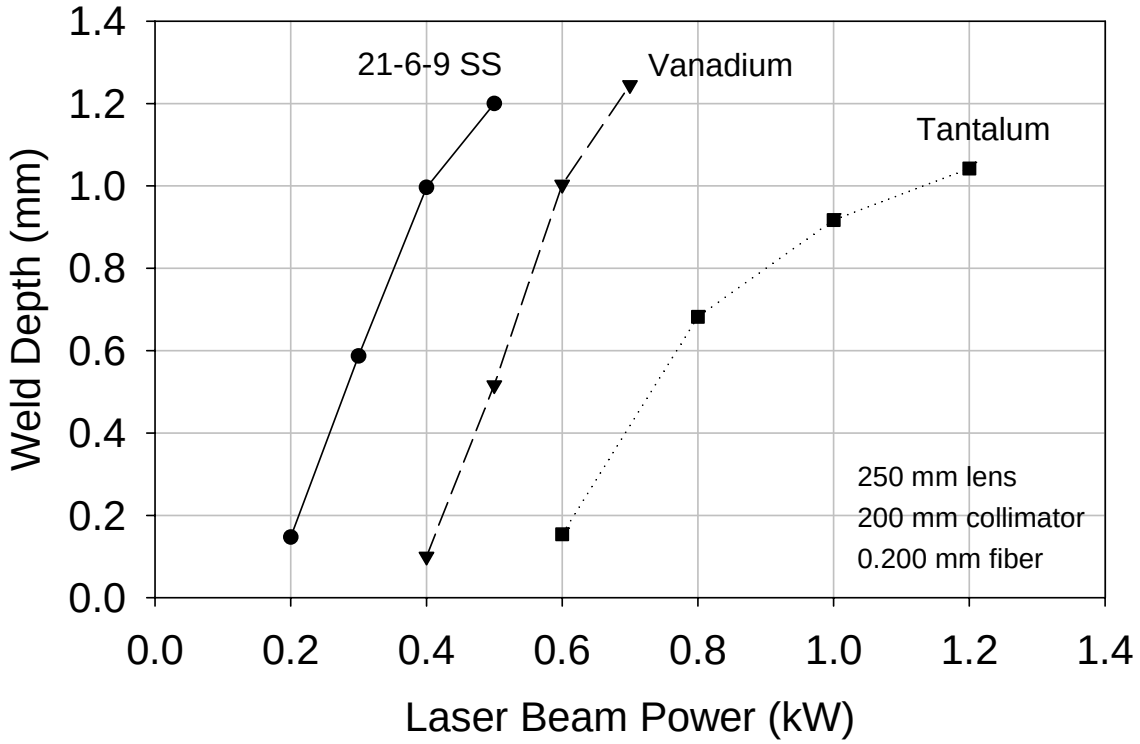


Figure 13. Measured weld depths and widths at the half-depth location for the 21-6-9SS, vanadium, and tantalum welds plotted as a function of laser beam power. All welds were made at a travel speed of 40 ipm.

# APPENDIX 1: Laser Beam Diagnostic Results

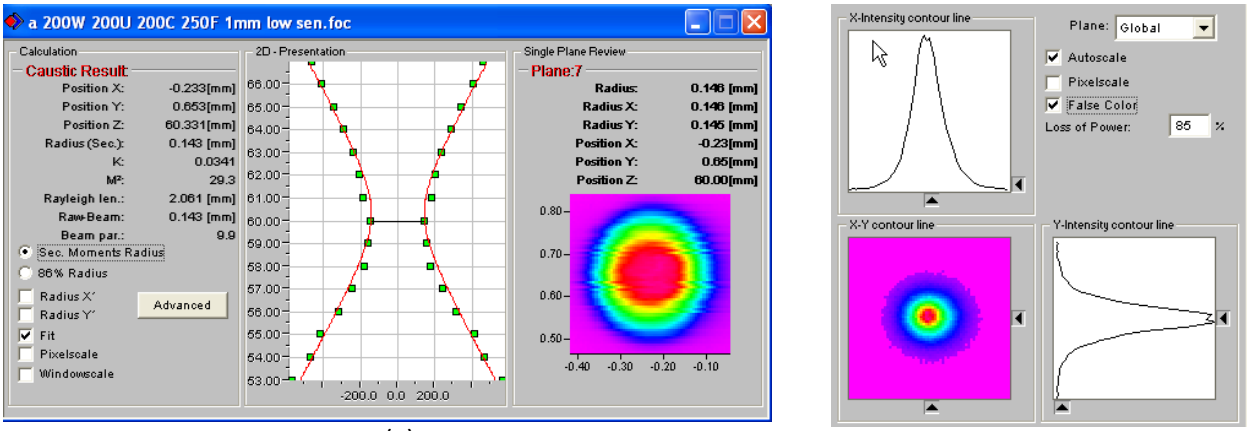


(a)

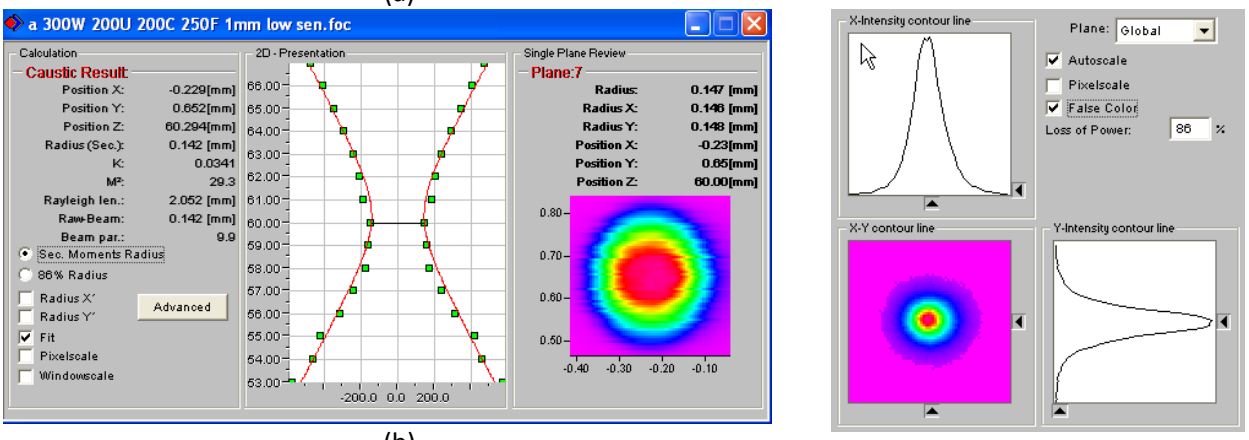


(b)

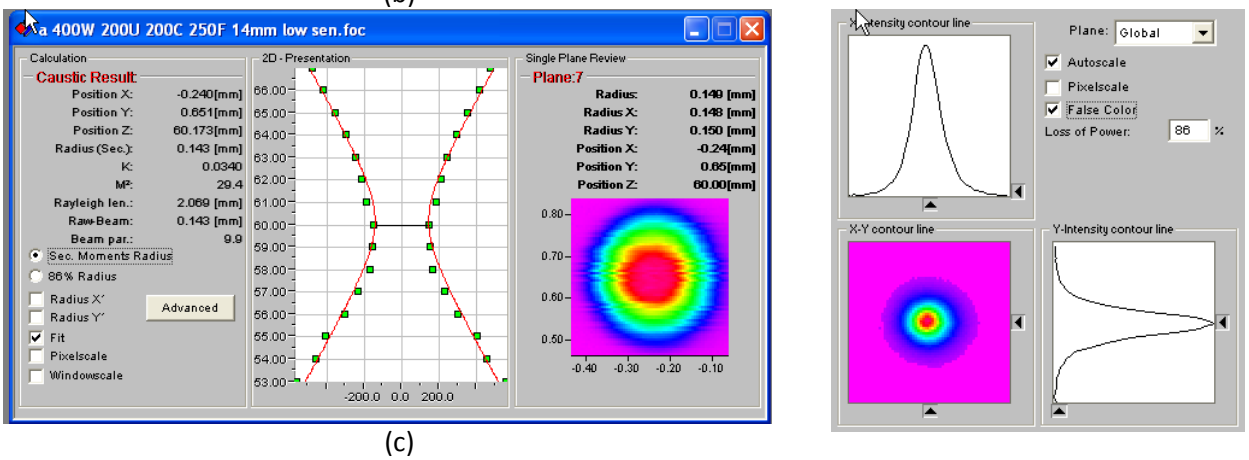


(c)

Figure A1. Laser beam diagnostic results for the flat plate welds, March 30, 2009. a) 200W beam, b) 300W beam, c) 400W beam. The caustic results are presented on the left hand side of the figure, and 2 orthogonal cross global sections through the beam are shown on the right hand side.

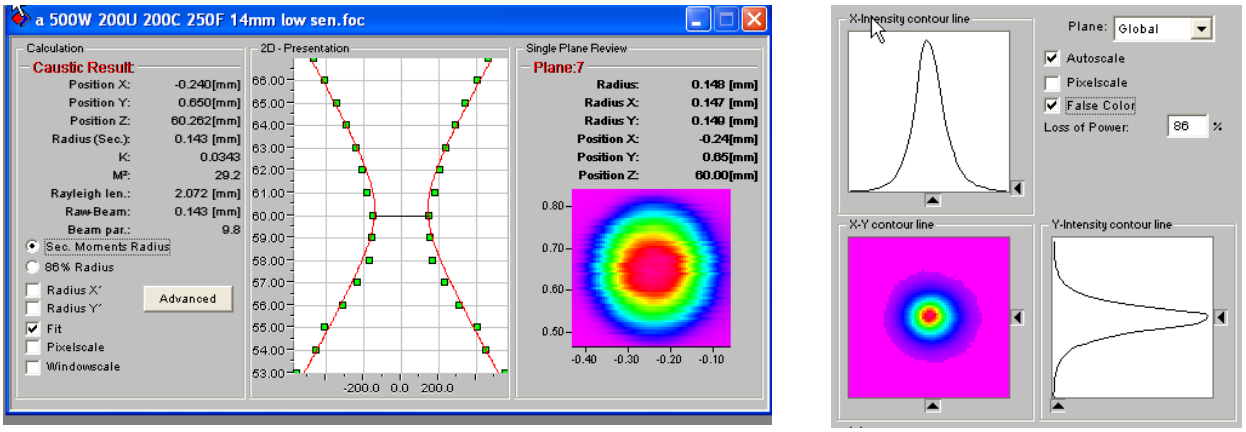


(d)

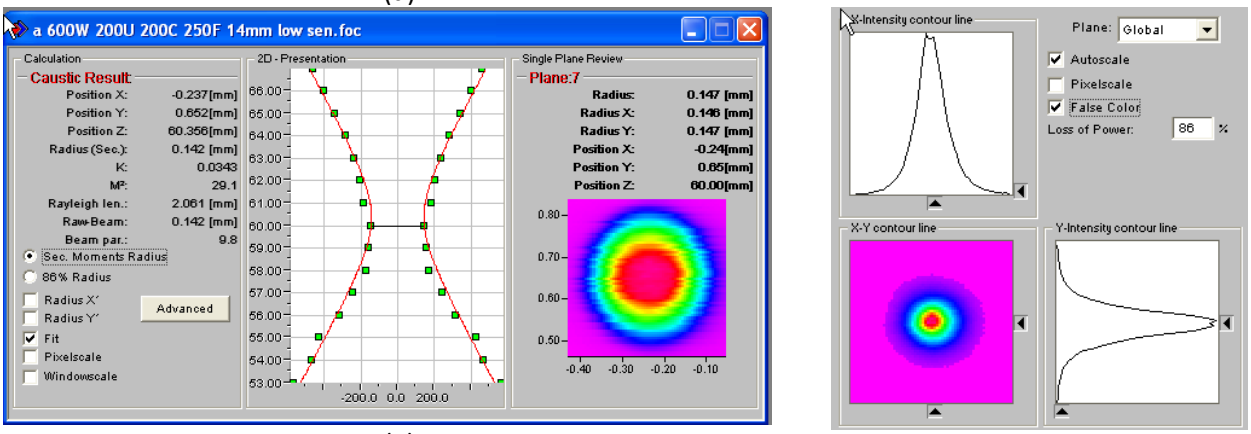


(e)

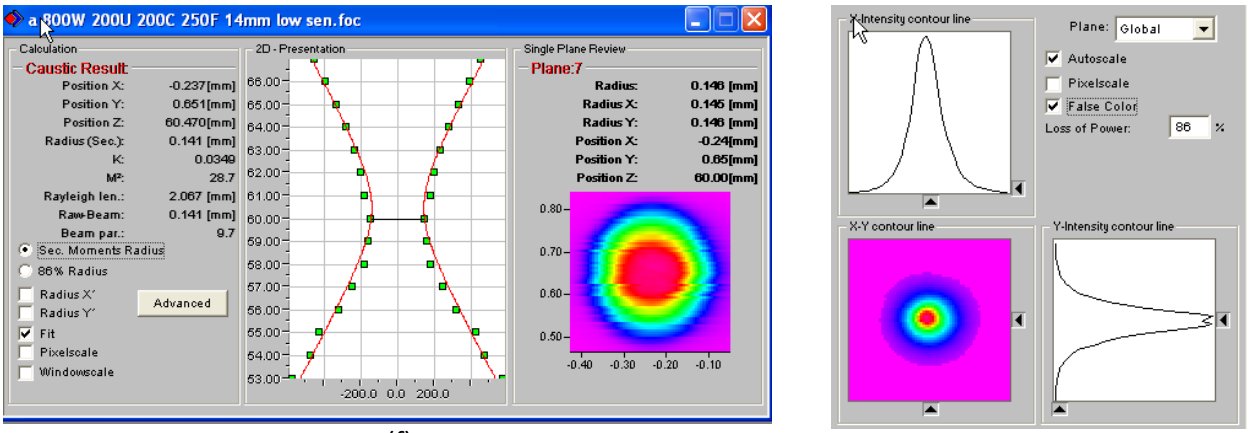


(f)

Figure A1 continued: d) 500W beam, e) 600W beam, f) 800W beam.

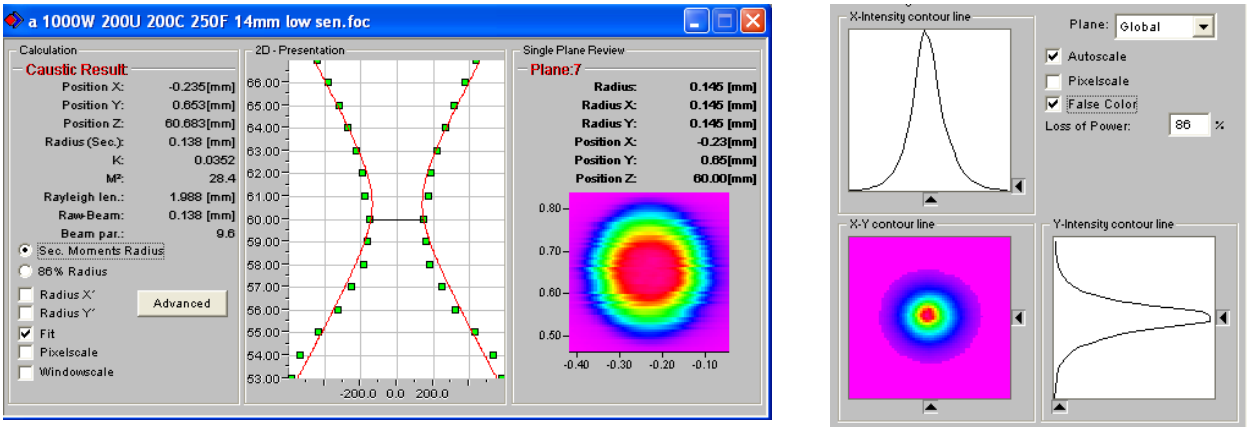


(g)

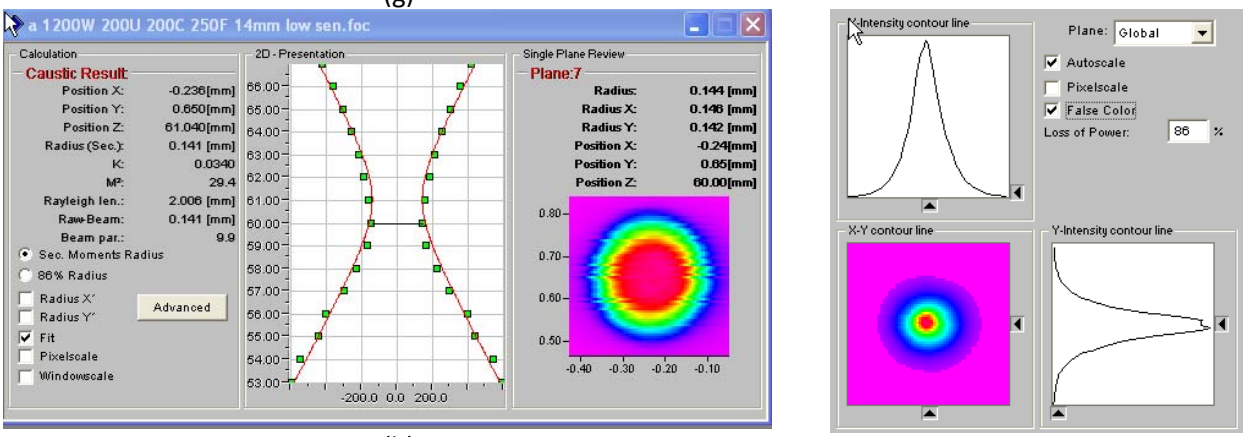


(h)

Figure A1 continued: g) 1000W beam, h) 1200W beam.